applied sciences

MDPI

Article

Adaptive Neural Network Control of Zero-Speed Vessel Fin Stabilizer Based on Command Filter

Ziteng Sun, Chao Chen * and Guibing Zhu

Maritime College, Zhejiang Ocean University, Zhoushan 316000, China; sunziteng0418@163.com (Z.S.); zhuguibing2003@163.com (G.Z.)

* Correspondence: chenchaogh@zjou.edu.cn; Tel.: +86-156-6866-7982

Abstract: This paper proposes a zero-speed vessel fin stabilizer adaptive neural network control strategy based on a command filter for the problem of large-angle rolling motion caused by adverse sea conditions when a vessel is at low speed down to zero. In order to avoid the adverse effects of the high-frequency part of the marine environment on the vessel rolling control system, a command filter is introduced in the design of the controller and a command filter backstepping control method is designed. An auxiliary dynamic system (ADS) is constructed to correct the feedback error caused by input saturation. Considering that the system has unknown internal parameters and unmodeled dynamics, and is affected by unknown disturbances from the outside, the neural network technology and nonlinear disturbance observer are fused in the proposed design, which not only combines the advantages of the two but also overcomes the limitations of the single technique itself. Through Lyapunov theoretical analysis, the stability of the control system is proved. Finally, the simulation results also verify the effectiveness of the control method.

Keywords: command filtering; input saturation; adaptive control; nonlinear disturbance observer; RBF neural network

Citation: Sun, Z.; Chen, C.; Zhu, G. Adaptive Neural Network Control of Zero-Speed Vessel Fin Stabilizer Based on Command Filter. *Appl. Sci.* **2022**, *12*, 754. https://doi.org/10.3390/app12020754

Academic Editor: Seong-Ik Han

Received: 11 November 2021
Accepted: 10 January 2022
Published: 12 January 2022

1. Introduction

Vessels in navigation operations may be easily disturbed by harsh environmental factors such as wind, waves, currents, etc., and violent rolling motions may threaten the life and safety of the vessel itself, which also may cause capsizing or other major accidents of vessel destruction and death [1]. In this context, scholars of the ocean engineering community have proposed many effective anti-rolling methods, such as installing bilge keels [2], using a rudder for stabilization [3], adding an anti-rolling tank [4], installing anti-rolling fins [5], etc. The works [6,7] pointed out that a bilge keel can reduce the roll angle of the vessel by about 20%, an anti-rolling tank can reduce the roll by up to 50%, and a rudder can reduce the roll by about 60%. In contrast, a fin stabilizer has the best anti-roll effect, which can reach about 85–90%. Therefore, many scholars have devoted their attention to fin stabilizers and proposed a variety of different control methods [8].

For the control issue of fin stabilizer, in the early stage, PID control based on Conolly's linear model [9] has a good anti-rolling effect for small-angle vessel rolling, and has been widely used. When the ship rolls at a large angle, the nonlinear characteristic of model parameters is inspired. However, the traditional PID control strategy is designed based on the Conolly linear model, which cannot have effective system nonlinear characteristics, so it is no longer applicable. To this end, scholars have introduced nonlinear control technology methods into the fin stabilizer control of vessel roll and proposed a series of control methods, such as sliding mode control [10,11], model predictive control [12], the Lyapunov direct method [13], and adaptive backstepping control [14]. In addition, the vessel rolling control system also needs to consider the uncertainties and actuator saturation. In view of the uncertainty of vessel rolling control systems, [15] used the fuzzy logic system to approximate the system uncertain parts and proposed a robust adaptive fuzzy control

scheme for vessel roll stabilization. In [16], a variable structure robust fin control scheme was proposed for vessel roll stabilization. In recent years, neural networks have been widely used in the control of nonlinear systems due to their good nonlinear approximation ability and self-learning ability. This neural network-based control strategy also plays an important role in the vessel's roll stabilization control. In [17], an adaptive control scheme based on a neural network and an adaptive backstepping method was proposed to overcome the uncertainties of the rolling control system. In [18], an RBF neural network is used to estimate the uncertainty, and a new type of fin stabilizer lift feedback adaptive control system is designed which effectively improves the anti-roll effect. In [19], an adaptive PID controller based on a BP neural network is designed. Through the prediction output of vessel roll angle, the self-tuning of PID controller parameters is realized by using the adaptive and nonlinear characteristics of a neural network. In [20], the combination of a wavelet neural network and the adaptive control design of a vessel fin stabilizer system effectively improved the shortcomings of the poor adaptability of conventional PID control, and the control system was shown to have good fault tolerance and strong nonlinear adaptability. Regarding the external uncertainty of the system, it is estimated by introducing a disturbance observer in [21–24]. Because of its unique advantages, the disturbance observer technique has also received much attention from scholars [25–27].

Another practical problem regarding the fin stabilizer equipped on vessels is of the physical constraint, i.e., input saturation, which is inevitable [28]. In a vessel rolling control system, when the fin angle is used as the control input of the system, it may occur that the actual control input cannot reach the ideal control input level, which affects the stability of the control system [29]. Therefore, it is necessary to consider the influence of input saturation in the design process of vessel rolling control. To handle the effect of input saturation, refs [30,31] used a gain-scheduling algorithm to deal with the input rate and amplitude saturation problem, which effectively improved the stability of vessel rolling control system. In [32], the adverse effect of input saturation on the adaptive capability of the system was effectively dealt with by designing an auxiliary dynamic system to correct the feedback error. For the issue of saturation constraint, there are several effective approaches, such as model augmentation [33], smooth function substitution [34], and augmented error signal (AES) [35].

Based on the above observations, this paper proposes a zero-speed vessel fin stabilizer adaptive neural network control strategy for the vessel rolling control problem in the presence of input saturation, dynamic uncertainty and external unknown disturbance. Firstly, an auxiliary dynamic system is constructed to prevent the adaptive capacity of the system from being destroyed by input saturation. Then, the neural network technology is employed to overcome the dynamic uncertainty of the system model, and the disturbance observer is used to estimate the external unknown disturbance. Considering that the model approximation ability of BP neural network is very dependent on learning samples and the convergence rate is slow, the number of hidden layer nodes of the wavelet neural network is difficult to determine. Furthermore, RBF neural networks have arbitrary approximation performance and optimal approximation performance in theory, and the learning convergence rate is fast; therefore, this paper selects an RBF neural network [6,34,36] to approximate the dynamic uncertainty of the system model. In addition, in engineering practice, due to the presence of high-frequency and low-frequency parts in the marine environment, the high-frequency parts may enter the vessel rolling motion control system. In this case, the roll angle caused by the high-frequency part will be polluted, and the backstepping method requires the derivative operation of the virtual control, which, in turn, will aggravate the adverse effects of the high-frequency part, making the control system unable to operate normally. Therefore, this research introduces command filtering technology in the design process to overcome the adverse effects of the high-frequency part of the ocean. The main contributions of this paper are as follows: (i) An auxiliary dynamic system (ADS) is designed to correct the feedback error to overcome the influence of input saturation on the adaptive ability of the system. (ii) A fusion of neural network technology and a nonlinear disturbance observer is designed for the dynamic uncertainty and external

unknown disturbance of the vessel's roll control system, which not only breaks through the requirements of the disturbance observer for the knowledge of the controlled object model from the design mechanism but also overcomes the fact that the neural network technology cannot effectively reconstruct external disturbance. (iii) The introduction of a unique command filtering method which combines command filtering with the backstepping method overcomes the problem that the adverse effects of the high-frequency part of the ocean on the control system are aggravated by the backstepping method of the derivation operation.

The purpose of this work is to reduce the vessel roll and achieve stabilization by the fin stabilizer for the zero-speed vessel, which is subject to unknown dynamic, ocean disturbance and input saturation. The work arrangement of this paper is as follows. Section 2 introduces the mathematical model and preliminary knowledge of vessel rolling motion. Section 3 proposes a zero-speed fin stabilizer adaptive neural network control strategy. Section 4 presents simulations to verify the effectiveness of the control method. Section 5 draws conclusions.

2. Problem Formulation and Preliminaries

2.1. Problem Formulation

In the application of vessel engineering, the mathematical models of vessel rolling motion mostly use the vessel rolling linear model based on the Conolly theory, which can better describe the vessel rolling motion when the vessel roll angle is small. However, when the vessel roll angle is too large, it will cause a nonlinear change of the parameters of the vessel rolling mathematical model and a nonlinear change of the rolling moment, which makes the vessel rolling linear model unable to accurately reflect the vessel motion. Therefore, this paper uses the nonlinear rolling mathematical model to describe the vessel rolling motion. The model is as follows [1]:

$$(I_{xx} + J_{xx})\ddot{\varphi} + \delta_N\dot{\varphi} + \delta_W\dot{\varphi}|\dot{\varphi}| + Dh\varphi\left[1 - (\varphi/\varphi_v)^2\right] = M_c + M_W \tag{1}$$

$$I_{xx} + J_{xx} = \frac{DB^2}{g}(0.3085 + \frac{0.0227B}{d} - \frac{0.0043L}{100})^2 \tag{2}$$

$$\delta_N = 2n_1\sqrt{Dh(I_{xx} + J_{xx})}/\pi \tag{3}$$

$$\delta_W = 3n_1(I_{xx} + J_{xx})/4 \tag{4}$$

$$M_c = -2L_fF_z \tag{5}$$

$$M_W = -Dha_e \tag{6}$$

where φ is the roll angle of the vessel, I_{xx} and J_{xx} are the inertia moment of the vessel and the additional inertia moment of the vessel, δ_N and δ_W are the damping coefficients, D is the displacement of the vessel, h is the initial metacentric height of the vessel, φ_v is the inlet angle of the vessel, M_c is the control moment of the vessel's fin stabilizer and M_W is the wave moment acting on the vessel. g is the acceleration of gravity, B is the width of the vessel, L is the length between the two perpendiculars of the vessel, d is the draft of the vessel, n_1 and n_2 are the experimental coefficients changing with the vessel, L_f is the righting arm, F_z is the rolling stability force generated on the fin stabilizer and a_e is the effective wave angle.

When the vessel is at low speed down to zero, the zero-speed fin stabilizer obtains the lift force acting on the fin by rapidly and actively tapping the water, i.e., the rolling stability force. If we choose a position where the distance between the fin axis and the leading edge is 1/5 chord length, the lift generated on the fin stabilizer at zero speed at this time is:

$$F_z = F_1 + F_2\cos\alpha \tag{7}$$

$$F_1 = 7.2(\gamma + x_0)^2(v - x_0)l\rho\omega\|\omega\|\sin\alpha + 11.58(\gamma + x_0)^2(v - x_0)l\rho\omega\|\omega\|\cos\alpha \quad (8)$$

$$F_2 = (12\gamma^2 v + v^3)l\rho\omega\|\omega\|/3 \quad (9)$$

$$x_0 = \gamma\kappa/1.3$$

where γ is the 1/4 fin chord length of the fin surface, v is the distance between the fin axis and the midpoint of the chord length, ω is the angular velocity of the fin, α is the angle of the fin, l is the span length of the fin type, ρ is the density of the fluid and κ is the thickness ratio of the fin type.

When the vessel is at anchor, the anchor chain forces caused by the sea disturbance influence the vessel roll. However, this paper studies roll stability of a vessel at low speed down to zero, so the influence of anchor chain force is not considered. In addition, the hydrodynamic forces are omitted in Equations (7)–(9). However, these forces can be regarded as unknown dynamics which can be reconstructed by the adaptive neural network and the disturbance observer.

According to (1)–(6), one can obtain

$$\ddot{\varphi} = a_1\varphi + a_2\varphi^3 + a_3\dot{\varphi} + a_4\dot{\varphi}|\dot{\varphi}| + bF_z + ca_e \quad (10)$$

$$a_1 = -\frac{Dh}{I_{xx} + J_{xx}} \quad (11)$$

$$a_2 = \frac{Dh}{(I_{xx} + J_{xx})\varphi_v{}^2} \quad (12)$$

$$a_3 = -\frac{\delta_N}{I_{xx} + J_{xx}} \quad (13)$$

$$a_4 = -\frac{\delta_W}{I_{xx} + J_{xx}} \quad (14)$$

$$b = -\frac{2L_f}{I_{xx} + J_{xx}} \quad (15)$$

$$c = -\frac{Dh}{I_{xx} + J_{xx}} \quad (16)$$

Let $\varphi = x_1$, $\dot{\varphi} = x_2$, which yields $x = [x_1 \quad x_2]^{\mathrm{T}} = [\varphi \quad \dot{\varphi}]^{\mathrm{T}}$. Let $u = F_z$, $d_e = ca_e$. In practical engineering applications, according to factors such as the structure of the vessel's fin stabilizer and the physical limitations of the power system and other factors, it can be known that the rolling stability force generated on the fin stabilizer will be constrained by input saturation. The nonlinearity of input saturation is described as follows:

$$u = u(v) = \begin{cases} u_{\max}, & v > u_{\max} \\ v, & u_{\min} \le v \le u_{\max} \\ u_{\min}, & v < u_{\min} \end{cases} \quad (17)$$

where v is the command control input, u is the actual control input, and $u_{\max} > 0$ and $u_{\min} < 0$ are the known maximum control input and minimum control input, respectively.

Then, we have

$$\begin{cases} \dot{x}_1 = x_2 \\ \dot{x}_2 = f(x_1, x_2) + bu + d_e \\ y = x_1 \end{cases} \quad (18)$$

where $f(x_1, x_2) = a_1x_1 + a_2{x_1}^3 + a_3x_2 + a_4x_2|x_2|$.

Assumption 1. *The unknown external disturbance d_e and its derivative $\dot{d}_e$ are bounded and satisfy $|d_e| \le \bar{d}_e$, $|\dot{d}_e| \le \bar{\dot{d}}_e$. $\bar{d}_e$ and $\bar{\dot{d}}_e$ are unknown positive constants.*

Assumption 2. *$f(x_1, x_2)$ and b are unknown, but the sign of b is known.*

Assumption 3. *The (10) is input-to-state stable (ISS).*

Remark 1. *Assumption 1 is formulated to ensure the feasibility of the designed control strategy, and a similar assumption is made in [35]. The inertia matrix in the vessel mathematical model can be obtained by semi-physical experiments, but the coefficients of parameters in the model cannot be obtained in this way. The vessel's mathematical model is vulnerable to disturbance, and model oscillation occurs. Therefore, $f(x_1, x_2)$ and b are unknown. Since the control gain has an upper bound of 0, the sign of b is known. In the case of input saturation, the stability of the device must be ensured in order to satisfy the global stability, so Assumption 3 is reasonable [37,38].*

The control objective of this paper is to find an adaptive neural network control law for the zero-speed vessel fin stabilizer control system (10), so that the output φ approaches the expected value y_d and ensures that all signals in the closed-loop control system are uniformly bounded.

2.2. Preliminaries

The radial basis function neural network (RBF NN) is described as follows:

$$f_N(x) = W^{\mathrm{T}}\psi(x) \tag{19}$$

where $W = [W_1, \cdots, W_m]^{\mathrm{T}} \in R^m$ is the weight vector of the neural network. $\psi(x) = [\psi_1(x), \cdots, \psi_m(x)]^{\mathrm{T}} \in R^m$ is the basis function vector of the neural network, which is generally represented by the following Gaussian function:

$$\psi_j(x) = \exp\left(-\frac{\|x - \zeta_j\|^2}{2\omega_j{}^2}\right), j = 1, \cdots, m \tag{20}$$

where $x = [x_1, \cdots, x_q]^{\mathrm{T}} \in \Omega_x \subset R^q$ is the input vector of the neural network, $\zeta_j = [\zeta_{j,1}, \cdots, \zeta_{j,q}]^{\mathrm{T}} \in R^q$ is the center of the Gaussian function, $\omega_j > 0$ is the width of the Gaussian basis function and m is the number of nodes in the hidden layer.

Lemma 1 ([39])**.** *If the number of nodes in the hidden layer of the neural network is sufficient, then the RBF neural network can theoretically approximate the continuous function $f(x) \in R$ defined on a compact set $\Omega_x \subset R^q$ with arbitrary precision, namely*

$$f(x) = W^{*\mathrm{T}}\psi(x) + \varepsilon, \forall x \in \Omega_x \tag{21}$$

where $W^* \in R^m$ is the ideal weight vector of the neural network and $\varepsilon \in R$ is the approximation error. W^* is the case in which $|\varepsilon|$ is minimized when the condition of $x \in \Omega_x \subset R^q$ is satisfied, defined as follows

$$W^* := \arg\min_{W \in R^q} \left\{ \sup_{x \in \Omega_x} \left| f(x) - W^{\mathrm{T}}\psi(x) \right| \right\} \tag{22}$$

Assumption 4. *The approximation error ε is bounded, and $|\varepsilon| \leq \bar{\varepsilon}$. $\bar{\varepsilon}$ is an unknown positive constant.*

3. Controller Design and Stability Analysis

In this section, an adaptive neural network fin stabilizer control law is designed for the fin stabilizer control system of zero-speed vessel with unknown control gain by combining adaptive neural network technology, nonlinear disturbance observer, ADS and command filter backstepping methods. The specific design process is as follows.

3.1. Control Law Design

As shown in (18), $f(x_1, x_2)$ is an unknown nonlinear function, which cannot be directly used for the design of control law. According to Lemma 1, the RBF neural network can be used to approximate the unknown function, i.e.,

$$f(x_1, x_2) = W^{*\mathrm{T}}\psi(x) + \varepsilon \tag{23}$$

where ε is the approximation error of the neural network, $|\varepsilon| \leq \bar{\varepsilon}$.

According to (17), (18) and (23), the vessel roll fin stabilizer control system can be written as follows:

$$\begin{cases} \dot{x}_1 = x_2 \\ \dot{x}_2 = W^{*\mathrm{T}}\psi(x) + bu + \mathrm{e} \\ y = x_1 \end{cases} \tag{24}$$

where $e = d_e + \varepsilon$.

To handle the effect of input saturation, the following ADS is designed:

$$\begin{cases} \dot{\lambda}_1 = \lambda_2 - \phi_1\lambda_1 \\ \dot{\lambda}_2 = \hat{b}\Delta u - \phi_2\lambda_2 \end{cases} \tag{25}$$

where λ_1 and λ_2 are the states of the ADS, the initial values of λ_1 and λ_2 are set to 0, ϕ_1 and ϕ_2 are the design parameters and are both greater than 0, Δu is the difference between the actual control input u and the command control input v, $\Delta u = u - v$, $\hat{b}$ is an estimate of b. Δu is the non-executable part caused by the physical constraint of actuator, which results in the control quality. In this work, we use the design idea of ADS to compensate the effect of Δu. From the whole system, the non-executable part Δu affects φ and $\dot{\varphi}$. In this context, the ADS (25) is designed to compensate the effect of Δu.

Using (25), the error variable is redefined as follows:

$$\begin{cases} z_1 = x_1 - \lambda_1 \\ z_2 = x_2 - \alpha_1 - \lambda_2 \end{cases} \tag{26}$$

where z_1 and z_2 are the error variables and α_1 is the state of the command filter.

Define the command filter as shown below:

$$\begin{cases} \dot{\alpha}_1 = \omega_n\alpha_2 \\ \dot{\alpha}_2 = -2\xi\omega_n\alpha_2 - \omega_n\left(\alpha_1 - \alpha_1^0\right) \end{cases} \tag{27}$$

where ω_n is a design parameter and has a value greater than 0, and $\xi \in (0, 1]$ is also a design parameter. The initial value of filter state α_1 should be the same as the initial value of virtual control law α_1^0, that is, $\alpha_1(0) = \alpha_1^0(0)$, and the initial value of filter state α_2 is set to 0.

According to (26), the error of the compensation is defined as follows:

$$\begin{cases} \bar{z}_1 = z_1 - s_1 \\ \bar{z}_2 = z_2 - s_2 \end{cases} \tag{28}$$

where $\bar{z}_1$ and $\bar{z}_2$ are the compensated error variables, and s_1 and s_2 are the compensated variables.

The derivation of the first compensating error variable of (28) is as follows:

$$\begin{aligned} \dot{\bar{z}}_1 &= \dot{z}_1 - \dot{s}_1 \\ &= \dot{x}_1 - \dot{\lambda}_1 - \dot{s}_1 \\ &= x_2 - \lambda_2 + \phi_1\lambda_1 - \dot{s}_1 \\ &= z_2 + \alpha_1 + \phi_1\lambda_1 - \dot{s}_1 \\ &= z_2 + \alpha_1 - \alpha_1^0 + \alpha_1^0 + \phi_1\lambda_1 - \dot{s}_1 \end{aligned} \tag{29}$$

where α_1^0 is the virtual control law to be designed and $\alpha_1 - \alpha_1^0$ is the filtering error generated by the command filter.

The filtering error compensation dynamic is designed as follows to eliminate the influence of the filtering error:

$$\dot{s}_1 = -k_1 s_1 + \alpha_1 - \alpha_1^0 \tag{30}$$

where k_1 is a design parameter and its value is greater than constant 0. The initial value of the compensation variable s_1 is set to constant 0.

From (29) and (30), it is obtained that

$$\dot{\bar{z}}_1 = z_2 + \alpha_1^0 + \phi_1 \lambda_1 + k_1 s_1 \tag{31}$$

Further, the virtual control law α_1^0 is designed as

$$\alpha_1^0 = -s_2 - k_1 z_1 - \phi_1 \lambda_1 \tag{32}$$

α_1^0 is the virtual control law, which is used to stabilize the error $\bar{z}_1$. According to the Lyapunov theorem and command filter design framework, α_1^0 is designed as the form of Equation (32).

Substituting (32) into (31), we get

$$\dot{\bar{z}}_1 = \bar{z}_2 - k_1 \bar{z}_1 \tag{33}$$

Choose the Lyapunov function as follows:

$$V_1 = \frac{1}{2}\bar{z}_1^2 \tag{34}$$

According to (33), the time derivative of V_1 is

$$\begin{aligned} \dot{V}_1 &= \bar{z}_1 \dot{\bar{z}}_1 \\ &= \bar{z}_1(\bar{z}_2 - k_1 \bar{z}_1) \\ &= -k_1 \bar{z}_1^2 + \bar{z}_1 \bar{z}_2 \end{aligned} \tag{35}$$

According to (24), (26) and (28), the time derivative of $\bar{z}_2$ is

$$\begin{aligned} \dot{\bar{z}}_2 &= \dot{z}_2 - \dot{s}_2 \\ &= \dot{x}_2 - \dot{\alpha}_1 - \dot{\lambda}_2 - \dot{s}_2 \\ &= W^{*\mathrm{T}} \psi(x) + bu + \mathrm{e} - \dot{\alpha}_1 - \dot{\lambda}_2 - \dot{s}_2 \end{aligned} \tag{36}$$

From (30), s_1 is the compensation dynamic of the filter error $\alpha_1 - \alpha_1^0$. However, there is not filter error since the control input u occurs. Therefore, the compensation dynamic s_2 is designed as follows:

$$\dot{s}_2 = -k_2 s_2 \tag{37}$$

where k_2 is the design parameter and is greater than 0.

Substituting (25) and (37) into (36), one has

$$\begin{aligned} \dot{\bar{z}}_2 &= W^{*\mathrm{T}} \psi(x) + bu + \mathrm{e} - \dot{\alpha}_1 - \hat{b}\Delta u + \phi_2 \lambda_2 + k_2 s_2 \\ &= \hat{b}u + \tilde{b}u - \hat{b}\Delta u + W^{*\mathrm{T}} \psi(x) + \mathrm{e} - \dot{\alpha}_1 + \phi_2 \lambda_2 + k_2 s_2 \\ &= \hat{b}v + \tilde{b}u + W^{*\mathrm{T}} \psi(x) + \mathrm{e} - \dot{\alpha}_1 + \phi_2 \lambda_2 + k_2 s_2 \\ &= \hat{b}v + \tilde{b}v + \tilde{b}\Delta u + W^{*\mathrm{T}} \psi(x) + \mathrm{e} - \dot{\alpha}_1 + \phi_2 \lambda_2 + k_2 s_2 \\ &= bv + \tilde{b}\Delta u + W^{*\mathrm{T}} \psi(x) + \mathrm{e} - \dot{\alpha}_1 + \phi_2 \lambda_2 + k_2 s_2 \end{aligned} \tag{38}$$

where $\tilde{b} = b - \hat{b}$.

Let $bv = v_f$, where v_f is the actual control law which is used to stabilize the error $\bar{z}_2$. According to the Lyapunov theorem and command filter design framework, v_f is designed as follows:

$$v_f = -\hat{W}^{\mathrm{T}}\psi(x) - \hat{e} + \dot{\alpha}_1 - \phi_2\lambda_2 - k_2 z_2 - \bar{z}_1 \tag{39}$$

Because of $v = \frac{1}{b}v_f$, let $\frac{1}{b} = \beta$. The estimated value of β is $\hat{\beta}$, and the actual control law is designed as follows:

$$\begin{aligned} v &= \hat{\beta}v_f \\ &= \hat{\beta}(-\hat{W}^{\mathrm{T}}\psi(x) - \hat{e} + \dot{\alpha}_1 - \phi_2\lambda_2 - k_2 z_2 - \bar{z}_1) \end{aligned} \tag{40}$$

The adaptive laws are as follows:

$$\dot{\hat{W}} = \Gamma\left(\bar{z}_2\psi(x) + L\hat{e}\psi(x) - \sigma_1\hat{W}\right) \tag{41}$$

$$\dot{\hat{\beta}} = \bar{z}_2 v_f - \sigma_2\hat{\beta} \tag{42}$$

$$\dot{\hat{b}} = \bar{z}_2\Delta u + L\hat{e}u - \sigma_3\hat{b} \tag{43}$$

where σ_1, σ_2, σ_3 are design parameters and all are greater than 0. $\hat{W}$ is the estimated value of ideal weight vector W^*, Γ is the learning rate of neural network, and $\hat{e}$ is the estimated value of total disturbance e. According to the idea of [40], the following nonlinear disturbance observer is constructed:

$$\begin{cases} \dot{D} = -L(x_1, x_2)D + L(x_1, x_2)(-\hat{W}^{\mathrm{T}}\psi(x) - \hat{b}u - p(x_2)) \\ \hat{e} = D + p(x_2) \\ \dot{p}(x_2) = L(x_1, x_2)\dot{x}_2 \end{cases} \tag{44}$$

Substituting (39) and (40) into (38) yields

$$\begin{aligned} \dot{\bar{z}}_2 &= b\hat{\beta}v_f + \tilde{b}\Delta u + {W^*}^{\mathrm{T}}\psi(x) + \mathrm{e} - \dot{\alpha}_1 + \phi_2\lambda_2 + k_2 s_2 \\ &= b(\beta - \tilde{\beta})v_f + \tilde{b}\Delta u + {W^*}^{\mathrm{T}}\psi(x) + \mathrm{e} - \dot{\alpha}_1 + \phi_2\lambda_2 + k_2 s_2 \\ &= v_f - b\tilde{\beta}v_f + \tilde{b}\Delta u + {W^*}^{\mathrm{T}}\psi(x) + \mathrm{e} - \dot{\alpha}_1 + \phi_2\lambda_2 + k_2 s_2 \\ &= -b\tilde{\beta}v_f + \tilde{b}\Delta u + \tilde{W}^{\mathrm{T}}\psi(x) + \tilde{e} - k_2\bar{z}_2 - \bar{z}_1 \end{aligned} \tag{45}$$

where $\tilde{e} = e - \hat{e}$, $\tilde{W} = W^* - \hat{W}$, $\tilde{b} = b - \hat{b}$ and $\tilde{\beta} = \beta - \hat{\beta}$.

The time derivative of $\hat{e}$ is as follows:

$$\dot{\hat{e}} = L\tilde{W}^{\mathrm{T}}\psi(x) + L\tilde{b}u + L\tilde{e} \tag{46}$$

Consider the following Lyapunov function as

$$V_2 = V_1 + \frac{1}{2}\bar{z}_2^2 + \frac{1}{2}\tilde{W}^{\mathrm{T}}\Gamma^{-1}\tilde{W} + \frac{1}{2}\tilde{e}^2 + \frac{|b|}{2}\tilde{\beta}^2 + \frac{1}{2}\tilde{b}^2 \tag{47}$$

According to (45), the time derivative of V_2 is

$$\begin{aligned}
\dot{V}_2 &= \dot{V}_1 + \bar{z}_2\dot{\bar{z}}_2 - \tilde{W}^{\mathrm{T}}\Gamma^{-1}\dot{\hat{W}} + \tilde{e}\dot{e} - \tilde{e}\dot{\hat{e}} - |b|\tilde{\beta}\dot{\hat{\beta}} - \tilde{b}\dot{\hat{b}} \\
&= \dot{V}_1 + \bar{z}_2\Big(\tilde{W}^{\mathrm{T}}\psi(x) + \tilde{e} - k_2\bar{z}_2 - \bar{z}_1 - b\tilde{\beta}v_f + \tilde{b}\Delta u\Big) - \tilde{W}^{\mathrm{T}}\Gamma^{-1}\dot{\hat{W}} \\
&+\tilde{e}\dot{e} - \tilde{e}\dot{\hat{e}} - |b|\tilde{\beta}\dot{\hat{\beta}} - \tilde{b}\dot{\hat{b}} \\
&= -k_1\bar{z}_1^2 - k_1\bar{z}_2^2 + \bar{z}_2\tilde{W}^{\mathrm{T}}\psi(x) + \bar{z}_2\tilde{e} - \bar{z}_2 b\tilde{\beta}v_f + \bar{z}_2\tilde{b}\Delta u - \tilde{W}^{\mathrm{T}}\Gamma^{-1}\dot{\hat{W}} \\
&+\tilde{e}\dot{e} - \tilde{e}\dot{\hat{e}} - |b|\tilde{\beta}\dot{\hat{\beta}} - \tilde{b}\dot{\hat{b}} \\
&\le -k_1\bar{z}_1^2 - k_1\bar{z}_2^2 + \bar{z}_2\tilde{W}^{\mathrm{T}}\psi(x) + \bar{z}_2\tilde{e} + \bar{z}_2|b|\tilde{\beta}v_f + \bar{z}_2\tilde{b}\Delta u - \tilde{W}^{\mathrm{T}}\Gamma^{-1}\dot{\hat{W}} \\
&+\tilde{e}\dot{e} - \tilde{e}\dot{\hat{e}} - |b|\tilde{\beta}\dot{\hat{\beta}} - \tilde{b}\dot{\hat{b}}
\end{aligned} \tag{48}$$

Substituting (46) into (48) yields

$$\begin{aligned}
\dot{V}_2 &\le -k_1\bar{z}_1^2 - k_1\bar{z}_2^2 + \bar{z}_2\tilde{W}^{\mathrm{T}}\psi(x) + \bar{z}_2\tilde{e} + \bar{z}_2|b|\tilde{\beta}v_f + \bar{z}_2\tilde{b}\Delta u - \tilde{W}^{\mathrm{T}}\Gamma^{-1}\dot{\hat{W}} \\
&+ \tilde{e}\dot{e} - \tilde{e}\Big(L\tilde{W}^{\mathrm{T}}\psi(x) + L\tilde{b}u + L\tilde{e}\Big) - |b|\tilde{\beta}\dot{\hat{\beta}} - \tilde{b}\dot{\hat{b}} \\
&\le -k_1\bar{z}_1^2 - k_1\bar{z}_2^2 + \bar{z}_2\tilde{W}^{\mathrm{T}}\psi(x) + \bar{z}_2\tilde{e} + \bar{z}_2|b|\tilde{\beta}v_f + \bar{z}_2\tilde{b}\Delta u - \tilde{W}^{\mathrm{T}}\Gamma^{-1}\dot{\hat{W}} \\
&+ \tilde{e}\dot{e} - L\tilde{e}\tilde{W}^{\mathrm{T}}\psi(x) - L\tilde{e}\tilde{b}u - L\tilde{e}^2 - |b|\tilde{\beta}\dot{\hat{\beta}} - \tilde{b}\dot{\hat{b}} \\
&\le -k_1\bar{z}_1^2 - k_1\bar{z}_2^2 + \tilde{W}^{\mathrm{T}}\Gamma^{-1}\Big(\Gamma\bar{z}_2\psi(x) - \Gamma Le\psi(x) + \Gamma L\hat{e}\psi(x) - \dot{\hat{W}}\Big) \\
&+ |b|\tilde{\beta}\Big(\bar{z}_2 v_f - \dot{\hat{\beta}}\Big) + \tilde{b}\Big(\bar{z}_2\Delta u - Leu + L\hat{e}u - \dot{\hat{b}}\Big) + \bar{z}_2\tilde{e} + \tilde{e}\dot{e} - L\tilde{e}^2
\end{aligned} \tag{49}$$

Substituting (41)–(43) into (49) yields

$$\begin{aligned}
\dot{V}_2 &\le -k_1\bar{z}_1^2 - k_1\bar{z}_2^2 + \sigma_1\tilde{W}^{\mathrm{T}}\hat{W} - Le\tilde{W}^{\mathrm{T}}\psi(x) + \sigma_2|b|\tilde{\beta}\hat{\beta} + \sigma_3\tilde{b}\hat{b} - Le\tilde{b}u \\
&+ \bar{z}_2\tilde{e} + \tilde{e}\dot{e} - L\tilde{e}^2 \\
&\le -k_1\bar{z}_1^2 - k_1\bar{z}_2^2 + \sigma_1\tilde{W}^{\mathrm{T}}\hat{W} + \Big|Le\tilde{W}^{\mathrm{T}}\psi(x)\Big| + \sigma_2|b|\tilde{\beta}\hat{\beta} + \sigma_3\tilde{b}\hat{b} + \big|Le\tilde{b}u\big| \\
&+ \bar{z}_2\tilde{e} + \tilde{e}\dot{e} - L\tilde{e}^2
\end{aligned} \tag{50}$$

According to the Young inequality, the following inequality holds:

$$\tilde{W}^{\mathrm{T}}\hat{W} \le \frac{1}{2}\|W\|^2 - \frac{1}{2}\|\tilde{W}\|^2 \tag{51}$$

$$\tilde{\beta}\hat{\beta} \le \frac{1}{2}\beta^2 - \frac{1}{2}\tilde{\beta}^2 \tag{52}$$

$$\tilde{b}\hat{b} \le \frac{1}{2}b^2 - \frac{1}{2}\tilde{b}^2 \tag{53}$$

$$Le\tilde{W}^{\mathrm{T}}\psi(x) \le \frac{1}{4}\|\tilde{W}\|^2 + \|Le\psi(x)\|^2 \tag{54}$$

$$Le\tilde{b}u \le \frac{1}{2}\tilde{b}^2 + \frac{1}{2}\|Leu\|^2 \tag{55}$$

$$\bar{z}_2\tilde{e} \le \frac{1}{2}\bar{z}_2^2 + \frac{1}{2}\tilde{e}^2 \tag{56}$$

$$\tilde{e}\dot{e} \le \frac{1}{2}\tilde{e}^2 + \frac{1}{2}\dot{e}^2 \tag{57}$$

Substituting (51)–(57) into (50) yields

$$\begin{aligned}\dot{V}_2 &\le -k_1\bar{z}_1^2 - k_2\bar{z}_2^2 + \frac{\sigma_1}{2}\|W\|^2 - \frac{\sigma_1}{2}\|\tilde{W}\|^2 + \frac{1}{4}\|\tilde{W}\|^2 + \|Le\psi(x)\|^2 + \frac{\sigma_2|b|}{2}\beta^2 \\ &- \frac{\sigma_2|b|}{2}\tilde{\beta}^2 + \frac{\sigma_3}{2}b^2 - \frac{\sigma_3}{2}\tilde{b}^2 + \frac{1}{2}\tilde{b}^2 + \frac{1}{2}\|Leu\|^2 + \frac{1}{2}\bar{z}_2^2 + \frac{1}{2}\tilde{e}^2 + \frac{1}{2}\tilde{e}^2 \\ &+ \frac{1}{2}\dot{e}^2 - L\tilde{e}^2 \\ &\le -k_1\bar{z}_1^2 - \left(k_2 - \frac{1}{2}\right)\bar{z}_2^2 - \left(\frac{\sigma_1}{2} - \frac{1}{4}\right)\|\tilde{W}\|^2 - (L-1)\tilde{e}^2 - \frac{\sigma_2|b|}{2}\tilde{\beta}^2 \\ &- \left(\frac{\sigma_3}{2} - \frac{1}{2}\right)\tilde{b}^2 + \frac{\sigma_1}{2}\|W\|^2 + \|Le\psi(x)\|^2 + \frac{\sigma_2|b|}{2}\beta^2 + \frac{\sigma_3}{2}b^2 \\ &+ \frac{1}{2}\|Leu\|^2 + \frac{1}{2}\dot{e}^2 \\ &\le -cV + M\end{aligned} \tag{58}$$

where $c = \min\left\{k_1, k_2 - \frac{1}{2}, \frac{\sigma_1}{2} - \frac{1}{4}, L-1, \frac{\sigma_2|b|}{2}, \frac{\sigma_3}{2} - \frac{1}{2}\right\}$, $M = \frac{\sigma_1}{2}\|W\|^2 + \|Le\psi(x)\|^2 + \frac{\sigma_2|b|}{2}\beta^2 + \frac{\sigma_3}{2}b^2 + \frac{1}{2}\|Leu\|^2 + \frac{1}{2}\dot{e}^2$.

3.2. Stability Analysis

Based on the above analysis, the main conclusions are given in the form of a theorem.

Theorem 1. *Considering the Assumptions 1–3,the control law (40) based on the virtual control law (32) and the parameter adaptation law (41)–(43) can ensure that the vessel fin stabilizer control system described by (10) has the following properties:*

(1) The closed-loop control system is stable and all signals of the closed-loop control system are ultimately uniformly bounded;

(2) When appropriate design parameters k_1, k_2, σ_1, σ_2, σ_3 and L are selected, the error $\varphi - y_d$ between the actual roll angle φ of the vessel roll control system and the expected roll angle y_d can converge to a small residual set;

(3) Under the influence of input saturation, the error $\varphi - y_d$ satisfies:

$$\lim_{t\to\infty}|\varphi - y_d| \le \sqrt{\frac{2M}{c}} + \frac{\bar{\Theta}}{\sqrt{2k_1 - 1}} + \sqrt{\frac{2}{\varphi_1}}|\Delta u| \tag{59}$$

where $\varphi_1 > 0$ and $\bar{\Theta} > \left|\alpha_1 - \alpha_1^0\right|$. The boundedness of α_1 and α_1^0 will be obtained through the following proof process.

Proof. Solving (58), one has

$$V_2(t) \le \frac{M}{c} + \left[V_2(0) - \frac{M}{c}\right]e^{-ct} \le \frac{M}{c} + V_2(0)e^{-ct} \tag{60}$$

where $V_2(0)$ is the initial value of V_2.

According to (60), we know that V_2 is bounded. Then, from (47), $\bar{z}_1$, $\bar{z}_2$, $\tilde{W}$, $\tilde{e}$, $\tilde{\beta}$ and $\tilde{b}$ are also bounded. Because of $\lim_{t\to\infty} e^{-ct} = 0$, and according to (47), the following equations hold:

$$\lim_{t\to\infty}|\bar{z}_1| \le \sqrt{\frac{2M}{c}} \tag{61}$$

$$\lim_{t\to\infty}|\bar{z}_2| \le \sqrt{\frac{2M}{c}} \tag{62}$$

Therefore, it can be concluded that $|\bar{z}_1|$ and $|\bar{z}_2|$ converge to the compact set $\Omega_{\bar{z}_1} = \left\{\bar{z}_1 \middle| |\bar{z}_1| \le \sqrt{2M/c}\right\}$ and $\Omega_{\bar{z}_2} = \left\{\bar{z}_2 \middle| |\bar{z}_2| \le \sqrt{2M/c}\right\}$ as $t \to \infty$, respectively. Since

$\tilde{W}$ is bounded, it follows that $\hat{W}$ is also bounded. Under Assumptions 1–3 and $e = d_e + \varepsilon$, both e and $\hat{e}$ are bounded. According to Theorem 2 in [41], the error variable $z_{b,1}$, the virtual control law $\bar{\alpha}_1$ and its time derivative $\dot{\bar{\alpha}}_1$ are bounded (its boundedness can be proved by the backstepping design method, and the detailed proof process can be referred to the appendix in literature [35]), i.e., $z_1 - z_{b,1}$, $\alpha_1 - \bar{\alpha}_1$, and $\alpha_2 - \dot{\bar{\alpha}}_1$ are also bounded. Thus, z_1, α_1, α_2 are bounded. Meanwhile, it follows from the boundedness of (28), (37) and $\bar{z}_2$ that z_2 is bounded. Based on the boundedness of z_1, $\bar{z}_1$ and (28), it can be proved that the compensation signal s_1 in (30) is bounded. According to (26) and Assumption 3, the state variable λ_1 in (25) is bounded, and the state variable α_1^0 in (32) is bounded. Therefore, it can be proved that the state variable λ_2 in (25) is bounded. In addition, the boundedness of control law v in (40) can also be determined. According to the input saturation, it can be determined that the actual control input u is bounded. From $\Delta u = u - v$, we can know that Δu is also bounded. Through the above analysis, all signals of the closed-loop system are bounded.

Let $\Theta = \alpha_1 - \alpha_1^0$; then, by the boundedness of α_1 and α_1^0, Θ is also bounded, that is, when $\forall t_f \in [0, t)$, $|\Theta| \leq \bar{\Theta}$ and $\bar{\Theta} > 0$ are satisfied. According to (28) and (30), we get $\dot{s}_1 = -k_1 s_1 + \bar{\Theta}$. Let $V_{s,1} = 0.5 s_1^2$. Then, the time derivative of $V_{s,1}$ is

$$\begin{aligned} \dot{V}_{s,1} &\leq -(k_1 - 0.5) s_1^2 + 0.5\bar{\Theta}^2 \\ &\leq -(2k_1 - 1) V_{s,1} + 0.5\bar{\Theta}^2 \end{aligned} \tag{63}$$

where $k_1 > 0.5$.

Solving (63), we have

$$\begin{aligned} V_{s,1}(t) &= \left[V_{s,1}(0) - \frac{0.5\bar{\Theta}^2}{2k_1 - 1} \right] e^{-(2k_1 - 1)t} + \frac{0.5\bar{\Theta}^2}{2k_1 - 1} \\ &\leq \frac{0.5\bar{\Theta}^2}{2k_1 - 1} + V_{s,1}(0) e^{-(2k_1 - 1)t} \end{aligned} \tag{64}$$

where $V_{s,1}(0)$ is the initial value of $V_{s,1}$. Because $\lim_{t \to \infty} e^{-(2k_1 - 1)t} = 0$, s_1 converges to the compact set $\Omega_s = \left\{ s_1 \middle| |s_1| \leq \bar{\Theta} / \sqrt{2k_1 - 1} \right\}$ when $t \to \infty$. It should be noted that the positive number $\bar{\Theta}$ is only used for stability analysis and not for controller design, so only $\bar{\Theta}$ is required to exist.

Next, in order to obtain the bounds of variables λ_1, λ_2, a Lyapunov function $V_\lambda = 0.5\lambda_1^2 + 0.5\lambda_2^2$ is constructed, and the time derivative is as follows:

$$\begin{aligned} \dot{V}_\lambda &= \lambda_1 \dot{\lambda}_1 + \lambda_2 \dot{\lambda}_2 \\ &= \lambda_1 \lambda_2 - \phi_1 \lambda_1^2 + \hat{b} \Delta u \lambda_2 - \phi_2 \lambda_2^2 \\ &\leq -(\phi_1 - 0.5)\lambda_1^2 - (\phi_2 - 0.5 - 0.25\hat{b}^2)\lambda_2^2 + |\Delta u|^2 \\ &\leq -\varphi_1 V_\lambda + |\Delta u|^2 \end{aligned} \tag{65}$$

where $\varphi_1 = \min\left\{ 2\phi_1 - 1, 2\phi_2 - 1 - 0.5\hat{b}^2 \right\}$, $\phi_1 > 0.5$, $\phi_2 > 0.5 + 0.25\hat{b}^2$.

Solving (65), one can get

$$V_\lambda(t) \leq \frac{|\Delta u|^2}{\varphi_1} + \left[V_\lambda(0) - \frac{|\Delta u|^2}{\varphi_1} \right] e^{-\varphi_1 t} \tag{66}$$

Since $\lambda(0) = 0$, the initial value of V_λ is $V_\lambda(0) = 0$. According to $V_\lambda = 0.5\lambda_1^2 + 0.5\lambda_2^2$ and (66), we have

$$|\lambda_1| \leq \sqrt{\frac{2}{\varphi_1}} |\Delta u| \tag{67}$$

$$|\lambda_2| \leq \sqrt{\frac{2}{\varphi_1}}|\Delta u| \tag{68}$$

From (26) and (28), one can get

$$|x_1 - \alpha_0| = |\bar{z}_1 + s_1 + \lambda_1| \leq |\bar{z}_1| + |s_1| + |\lambda_1| \tag{69}$$

where $\alpha_0 = y_d$.

Combining (61), (64), (67) and (69), there is

$$\lim_{t\to\infty} |x_1 - \alpha_0| \leq \sqrt{\frac{2M}{c}} + \frac{\bar{\Theta}}{\sqrt{2k_1 - 1}} + \sqrt{\frac{2}{\varphi_1}}|\Delta u| \tag{70}$$

According to (28), (62), (68) and $\dot{s}_2 = -k_2 s_2$, we have

$$\lim_{t\to\infty} |x_2 - \alpha_1| \leq \sqrt{\frac{2M}{c}} + \sqrt{\frac{2}{\varphi_1}}|\Delta u| \tag{71}$$

Therefore, from (70) and (71), we know that $x_1 - \alpha_0$ and $x_2 - \alpha_1$ are bounded. According to $x_1 = \varphi$, $\alpha_0 = y_d$ and (70), it can be obtained that when appropriate design parameters k_1, k_2, σ_1, σ_2, σ_3 and L are selected, $|\varphi - y_d|$ can converge to a very small value. At the same time, the error $\varphi - y_d$ satisfies (59). Theorem 1 has been proved. □

4. Simulation

This section takes a vessel as the simulation object to verify the effectiveness of the designed control strategy. The displacement of the vessel is 1458 t, the length between the two perpendiculars of the vessel is 98 m, the width of the vessel is 10.2 m, the draft depth of the vessel is 3.1 m, the fin force arm of the fin stabilizer is 3.46 m, the flooding angle of the vessel is 0.75 rad and the initial metacentric height of the vessel is 1.15 m. The experimental coefficients n_1 and n_2 varying with the vessel are 0.031 and 0.0152, respectively. The span of the fin stabilizer is 1.8 m, the chord length is 2.5 m, the thickness ratio is 0.2, and the density of water is set to 1020 kg/m^3. The working angle of the fin stabilizer at zero speed is between $\pm$1.05 rad and the maximum rotation speed is 0.79 rad/s. By using the above parameters for the calculation, the relevant parameters of the vessel rolling motion mathematical model can be obtained as follows: $a_1 = -0.7542$, $a_2 = 1.3403$, $a_3 = -0.0171$, $a_4 = -0.0114$, $c = -0.7542$.

The design parameters in the simulation are as follows: The initial value of the roll angle is 0.6 rad, the initial value of the angular velocity is 0 rad/s, and the expected output y_d is 0 rad.The number of hidden layer nodes m of the RBF neural network is 30, the center point ζ_j of the Gaussian function is evenly distributed on $[-2, 2] \times [-2, 2]$, the width ω_j is 0.8, the learning rate Γ is $0.00001 I_{30\times 30}$, and $I_{30\times 30}$ is an identity matrix with a dimension of 30. $W(0) = 0$, $s_1(0) = 0$, $s_2(0) = 0$, $\lambda_1(0) = 0$, $\lambda_2(0) = 0$, $\sigma_1 = 0.5$, $\sigma_2 = 0.000001$, $\sigma_3 = 0.00001$, $L = 5$, $\phi_1 = 1$, $\phi_2 = 1.5$, $\omega_n = 100$, $\xi = 0.9$, $k_1 = 3$, $k_2 = 60$, $\alpha_1 = -1.8$, $\alpha_1^0 = -1.8$, $\alpha_2 = 0$ and the disturbance e is $0.1sin(0.5t) - 0.11cos(0.35t) + 0.2sin(0.4t)$.

In order to further verify the superiority of the proposed control strategy in roll reduction, it is compared with the adaptive neural network control strategy without command filters. The virtual control law and control law are as follows:

$$\alpha_1 = -c_1 z_1 \tag{72}$$

$$v = \frac{1}{b}(-c_2 z_2 - z_1 - \hat{W}^{\mathrm{T}}\psi(x) + \dot{\alpha}_1) \tag{73}$$

$$\dot{\hat{W}} = \Gamma(z_2\psi(x) - \sigma\hat{W}) \tag{74}$$

In simulation, $c_1 = 0.5$, $c_2 = 1$, $b = -0.031$, $\Gamma = 0.00001 I_{30\times30}$, $\sigma = 0.005$. The other parameters are consistent with those in the scheme of this paper.

The simulation results under the control proposed scheme in this paper and the compared control schemes are shown in Figure 1. In Figure 1, φ, α, $\hat{e}$, ω, and F_z are the simulation results of the control strategy designed in this paper, and φ^*, α^*, $\hat{e}^*$, ω^*, ${F_z}^*$ are the simulation results of the same simulation objects in the compared control strategies, respectively. From Figure 1a, it can be seen that under both control strategies, the vessel's roll angle φ and φ^* can quickly approach the stabilization angle y_d in a short time and reach a stable state. However, after enlarging the image, it is obvious that the control scheme designed in this paper has a better roll reduction effect and smaller roll angle after the system is stable. In Figure 1b, the changes of fin angle α and α^* during operation are shown. It can be seen from the image that the fin angle of the contrast control scheme is larger than that of the control scheme in this paper at the same time, which is more biased in the positive direction of fin angle motion. In Figure 1c, the curve of the estimated disturbance $\hat{e}$, $\hat{e}^*$ and the actual disturbance e almost completely coincide, indicating that both control strategies have good estimation performance for unknown disturbances. Figure 1d is the fin angular velocity ω and ω^*. From Figure 1e, it is known that at the beginning, in order to resist the large angle rolling of the vessel, a large roll stability force was generated. When the vessel tends to be stable, the roll stability force F_z and ${F_z}^*$ also tend to be stable. Figure 1f shows the trajectory of the estimate of control gain $\hat{b}$ and the estimate of control gain reciprocal $\hat{\beta}$. From the graph, we can see that the value of the control gain is around 0.03 and the value of the inverse of the control gain is around 34. Based on the above simulation results, the zero-speed vessel fin stabilizer control system designed in this paper can quickly reduce the roll angle and restore the vessel to a stable state when large angle rolling occurs; therefore, it has good control performance.

To further verify the effectiveness of the proposed scheme, a simulation comparison with the conventional PID is carried out under two different ocean conditions. In case 1, the ocean disturbance is set as $e = 0.1sin(0.5t) - 0.11cos(0.35t) + 0.2sin(0.4t)$; in case 2, the ocean disturbance is set as $e = 0.5sin(0.5t) - 1.1cos(0.35t) + 2sin(0.4t)$. In simulation, the control gains of PID are set as $k_p = 10$, $k_i = 1$, $k_d = 10000$. The simulation results are shown in Figure 2.

From Figure 2a, it can be seen that the control performance under two control laws is almost identical, which indicates that the conventional PID can also ensure the stability of the closed-loop control system and achieve satisfying control performance. However, Figure 2b shows that the control performance degenerates when the ocean disturbance is magnified, and that the proposed control scheme in this work shows the advantage of robustness and adaptive ability.

The simulation comparison indicates that, compared with the conventional PID, the proposed adaptive NN-based disturbance observer control scheme is of strong robustness against the system dynamic and external disturbance, which attributes to the adaptive NN and disturbance observer techniques. Due to the adaptive ability, the proposed control scheme does not need to adjust the control gains repeatedly. Such an advantage is absent in the conventional PID, which needs to repeatedly adjust gain to restrain the time-vary ocean environmental, since it is not endowed with the adaptive ability.

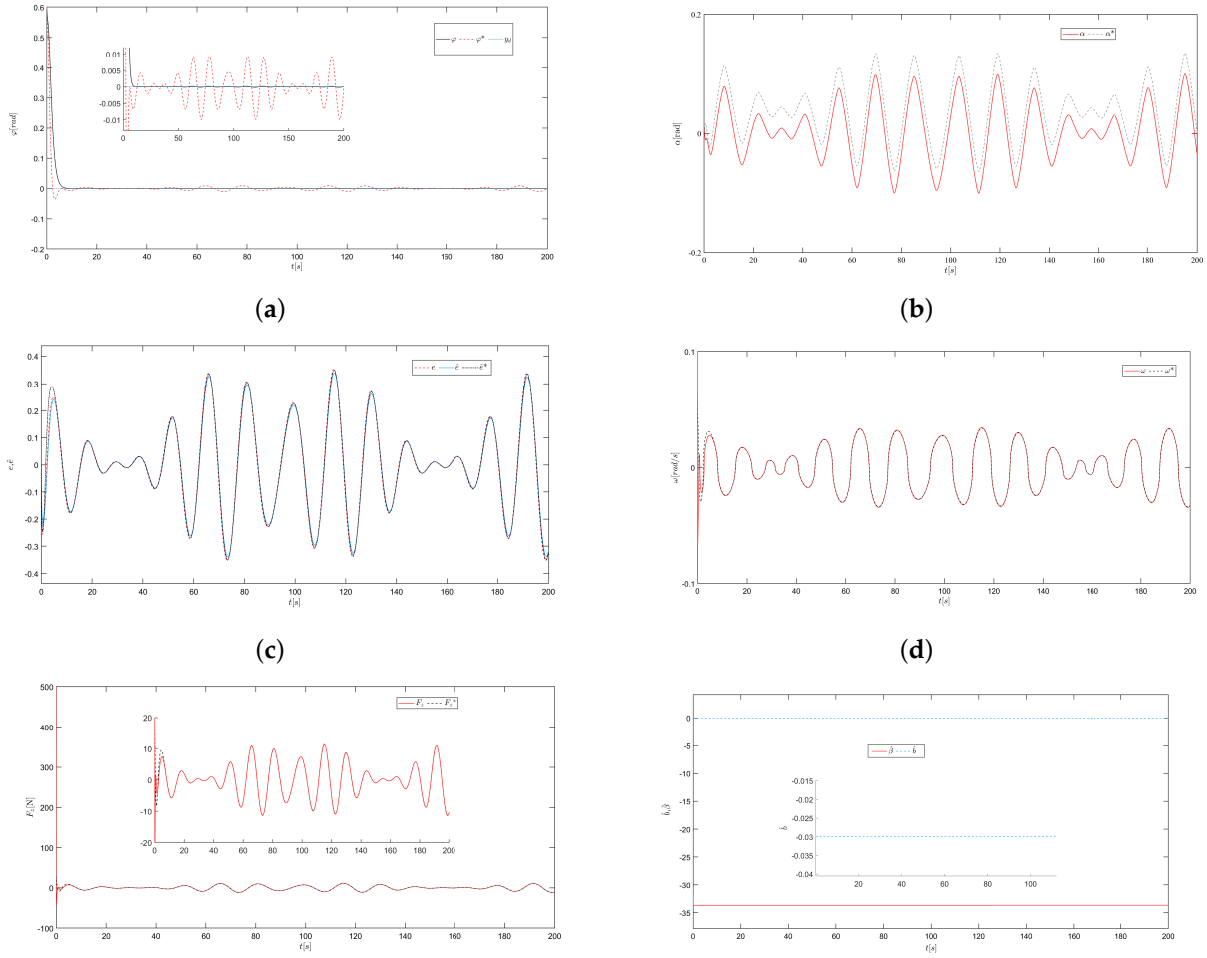

Figure 1. (**a**) Vessel's roll angle φ. (**b**) Fin angle α. (**c**) Disturbance e and estimated disturbance $\hat{e}$. (**d**) Fin angular velocity ω. (**e**) Rolling stability force F_z. (**f**) Estimation of control gain.

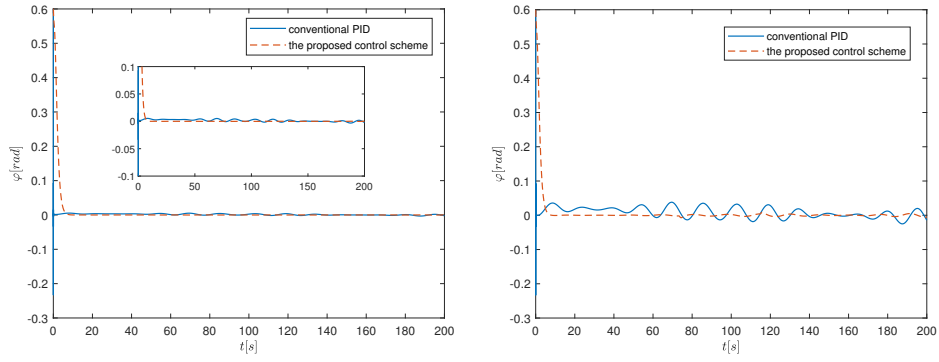

Figure 2. (**a**) The simulation comparison in case 1. (**b**) The simulation comparison in case 2.

5. Conclusions

In this paper, an adaptive neural network control scheme for the fin stabilizer of a zero-speed vessel based on a command filter for a large-angle roll of a zero-speed vessel under severe sea conditions is designed by combining ADS, a nonlinear disturbance observer, adaptive neural network technology and a command filter backstepping method. Through the fusion design of an RBF neural network and a nonlinear disturbance observer, the design mechanism breaks through the requirements of disturbance observer for the

controlled object model knowledge and overcomes the defects of neural network technology that cannot effectively reconstruct external disturbances. In the design process of the backstepping method, the command filter is introduced to overcome the possible adverse effects caused by the high-frequency part of the marine environment entering the control system. The robustness of the system is improved. The effectiveness of the designed control scheme is verified by simulation analysis.

In this work, we deliver a control system solution, which is not verified in the practical application of fin stabilizers and the results have not been verified. From the perspective of modeling, it is also important to take the wave and vessel's parameters into account to identify the range of resonance frequency. In addition, when the vessel is at anchor, the anchor chain forces caused by the sea disturbance influence the vessel roll, so the anchor chain forces should also be considered in modeling. In future studies, we will take these conditions into consideration.

Author Contributions: G.Z. designed the research ideas; Z.S. conducted theoretical research and simulation verification; G.Z. and C.C. conducted reliability analysis of the research results; C.C. provided financial support; Z.S. wrote this paper. All authors have read and agreed to the published version of the manuscript.

Funding: This work was supported by the National Science Foundation of Zhejiang Province under Grant LY21E090005.

Institutional Review Board Statement: Not applicable.

Informed Consent Statement: Not applicable.

Data Availability Statement: Not applicable.

Conflicts of Interest: The authors declare no conflict of interest.

Abbreviations

The following abbreviations are used in this manuscript:

ADS	Auxiliary dynamic system
RBF	Radial basis function
NN	Neural network
PID	Proportion integral differential
AES	Augmented error signal
ISS	Input-to-state stable

References

1. Li, R.; Li, T.; Bai, W.; Du, X. An adaptive neural network approach for ship roll stabilization via fin control. *Neurocomputing* **2016**, *173*, 953–957. [CrossRef]
2. Baniela, S.I. Roll motion of a ship and the roll stabilising effect of bilge keels. *J. Navig.* **2008**, *61*, 667–686. [CrossRef]
3. Zhao, J.; Liang, C.; Zhang, X. Rudder roll stabilization based on arc tangent nonlinear feedback for ships. *J. Mar. Sci. Eng.* **2020**, *8*, 245. [CrossRef]
4. Subramanian, R.; Jyothish, P.V. Genetic algorithm based design optimization of a passive anti-roll tank in a sea going vessel. *Ocean Eng.* **2020**, *203*, 107216. [CrossRef]
5. Luo, W.; Hu, B.; Li, T. Neural network based fin control for ship roll stabilization with guaranteed robustness. *J. Abbr.* **2017**, *230*, 210–218. [CrossRef]
6. Jiguang, S.; Lihua, L.; Zhang, S.; Wang, J. Design and experimental investigation of a GA-based control strategy for a low-speed fin stabilizer. *Ocean Eng.* **2020**, *218*, 108234. [CrossRef]
7. Alarçin, F.; Demirel, H.; Su, M.E.; Yurtseven, A. Modified pid control design for roll fin actuator of nonlinear modelling of the fishing boat. *Pol. Marit. Res.* **2014**, *1*, 3–8. [CrossRef]
8. Liang, L.; Zhao, P.; Zhang, S.; Ji, M.; Song, J.; Yuan, J. Simulation and experimental study on control strategy of zero-speed fin stabilizer based on disturbance and compensation. *PLoS ONE* **2018**, *13*, e0204446. [CrossRef]
9. Hickey, N.A.; Grimble, M.J.; Johnson, M.A.; Katebi, M.R.; Melville, R. Robust fin roll stabilisation of surface ships. In Proceedings of the 36th IEEE Conference on Decision and Control, San Diego, CA, USA, 12 December 1997; Volume 5, pp. 4225–4230.
10. Koshkouei, A.J.; Law, Y.; Burnham, K.J. Sliding mode and PID controllers for ship roll stabilisation: A comparative simulation study. *IFAC Proc. Vol.* **2005**, *38*, 7–12. [CrossRef]

11. Jin, Z.;Zhang, W.; Liu, S.; Gu, M. Command-filtered backstepping integral sliding mode control with prescribed performance for ship roll stabilization. *Appl. Sci.* **2019**, *9*, 4288. [CrossRef]
12. Perez, T.; Goodwin, G.C. Constrained predictive control of ship fin stabilizers to prevent dynamic stall. *Control Eng. Pract.* **2008**, *16*, 482–494. [CrossRef]
13. Karakas, S.; Ucer, E.; Pesman, E. Control design of fin roll stabilization in beam seas based on Lyapunov's direct method. *Pol. Marit. Res.* **2012**, *19*, 25–30. [CrossRef]
14. Xu, H.; Oliveira, P.; Soares, C.G. L1 adaptive backstepping control for path-following of underactuated marine surface ships. *Eur. J. Control* **2021**, *58*, 357–372. [CrossRef]
15. Yang, Y.; Zhou, C.; Jia, X. Robust adaptive fuzzy control and its application to ship roll stabilization. *Inf. Sci.* **2002**, *142*, 177–194. [CrossRef]
16. Yang, Y.; Jiang, B. Variable structure robust fin control for ship roll stabilization with actuator system. In Proceedings of the 2004 American Control Conference, Boston, MA, USA, 30 June–2 July 2004; Volume 6, pp. 5212–5217.
17. Bai, W.; Li, T.; Li, R. Neural network based direct adaptive for fin stabilizer system with input saturation. *Mar. Eng. Front.* **2013**, *1*, 63–68.
18. Sun, M.; Luan, T.; Liang, L. RBF neural network compensation-based adaptive control for lift-feedback system of ship fin stabilizers to improve anti-rolling effect. *Ocean Eng.* **2018**, *163*, 307–321. [CrossRef]
19. Ping, Y.U. Study of fin stabilizer's control system based on neural network for nonlinear roll motion of ship. *Inf. Control* **2003**, *3*, 264–267.
20. Hui, L.; Chen, G.; Jin, H. Design of adaptive inverse mode wavelet neural network controller of fin stabilizer. *Int. Conf. Neural Netw. Brain* **2005**, *3*, 1745–1748.
21. Zhang, Y.T.; Shi, W.R.; Qiu, M.B. Sliding backstepping control for fin stabilizer with nonlinear disturbance observer. *Control Decis.* **2010**, *25*, 1255–1260.
22. Liang, L.; Wen, Y. Disturbance compensation model predictive control for integrated rudder/fin roll stabilization. In Proceedings of the 2018 37th Chinese Control Conference (CCC), Wuhan, China, 25–27 July 2018; pp. 3859–3864.
23. Gong, S.; Song, L.; Tian, Y. PID control to rudder roll damping based on disturbance observer. *Mar. Electr. Electron. Eng.* **2005**, *33*, 23–26.
24. Han, Y. Neural disturbance observer based sliding mode control and its application to yaw/roll joint stabilization. *J. Comput. Inf. Syst.* **2014**, *10*, 7399–7406.
25. Chen, W.-H. Disturbance observer based control for nonlinear systems. *IEEE/ASME Trans. Mechatron.* **2004**, *9*, 706–710. [CrossRef]
26. Wu, J.; Huang, J.; Wang, Y.; Xing, K. Nonlinear disturbance observer-based dynamic surface control for trajectory tracking of pneumatic muscle system. *IEEE Trans. Control Syst. Technol.* **2013**, *22*, 440–455. [CrossRef]
27. Yang, J.; Li, S.; Yu, X. Sliding-mode control for systems with mismatched uncertainties via a disturbance observer. *IEEE Trans. Ind. Electron.* **2012**, *60*, 160–169. [CrossRef]
28. Lihua, L.; Peng, Z.; Songtao, Z.; Jia, Y. Simulation analysis of fin stabilizers on turning circle control during ship turns. *Ocean Eng.* **2019**, *173*, 174–182. [CrossRef]
29. Shao, K.; Tang, R.; Xu, F.; Wang, X.; Zheng, J. Adaptive sliding mode control for uncertain Euler–Lagrange systems with input saturation. *J. Frankl. Inst.* **2021**, *358*, 8356–8376. [CrossRef]
30. Lauvdal, T.; Fossen, T.I. Rudder roll stabilization of ships subject to input rate saturation using a gain scheduled control law. *IFAC Proc. Vol.* **1998**, *30*, 111–116. [CrossRef]
31. Ge, D.; Gao, Q.; Li, A.; Chen, Y. Rudder roll stabilization for ships with generalized predictive control based on fuzzy gain scheduler. In Proceedings of the 2009 IEEE International Conference on Intelligent Computing and Intelligent Systems, Shanghai, China, 20–22 November 2009; Volume 2, pp. 426–429.
32. Esmailian, E.; Farzanegan, B.; Menhaj, M.B.; Ghassemi, H. A robust neuro-based adaptive control system design for a surface effect ship with uncertain dynamics and input saturation to cargo transfer at sea. *Appl. Ocean. Res.* **2018**, *74*, 59–68. [CrossRef]
33. Zheng, Z.; Huang, Y.; Xie, L.; Zhu, B. Adaptive trajectory tracking control of a fully actuated surface vessel with asymmetrically constrained input and output. *IEEE Trans. Control. Syst. Technol.* **2017**, *26*, 1851–1859. [CrossRef]
34. Zhu, G.; Ma, Y.; Li, Z.; Malekian, R.; Sotelo, M. Event-triggered adaptive neural fault-tolerant control of underactuated msvs with input saturation. *IEEE Trans. Intell. Transp. Syst.* **2021**, 1–13. [CrossRef]
35. Zhu, G.; Du, J.; Kao, Y. Command filtered robust adaptive NN control for a class of uncertain strict-feedback nonlinear systems under input saturation. *J. Frankl. Inst.* **2018**, *355*, 7548–7569. [CrossRef]
36. Bai, W.; Li, T.; Gao, X.; Myint, K.T. Neural network based direct adaptive backstepping method for fin stabilizer system. In *International Symposium on Neural Networks*; Springer: Berlin/Heidelberg, Germany, 2013; pp. 212–219.
37. Wen, C.; Zhou, J.; Liu, Z.; Su, H. Robust adaptive control of uncertain nonlinear systems in the presence of input saturation and external disturbance. *IEEE Trans. Autom. Control* **2011**, *56*, 1672–1678. [CrossRef]
38. Zhou, J.; Wen, C. Robust adaptive control of uncertain nonlinear systems in the presence of input saturation. *IFAC Proc. Vol.* **2006**, *39*, 149–154. [CrossRef]
39. Liu, Q.; Li, D.; Ge, S.S.; Ji, R.; Ouyang, Z.; Tee, K.P. Adaptive bias RBF neural network control for a robotic manipulator. *Neurocomputing* **2021**, *447*, 213–223. [CrossRef]

40. Liu, S.; Liu, Y.; Wang, N. Nonlinear disturbance observer-based backstepping finite-time sliding mode tracking control of underwater vehicles with system uncertainties and external disturbances. *Nonlinear Dyn.* **2017**, *88*, 465–476. [CrossRef]
41. Farrell, J.A.; Polycarpou, M.; Sharma, M.; Dong, W. Command filtered backstepping. *IEEE Trans. Autom. Control* **2009**, *54*, 1391–1395. [CrossRef]